Neuronal Detection Triggers Systemic Digestive Shutdown in Response to Adverse Food Sources

Yating Liu[#], Guojing Tian[#], Ziyi Wang, Junkang Zheng, Huimin Liu, Sucheng Zhu, Zhao Shan*, Bin Qi*

Southwest United Graduate School, Yunnan Key Laboratory of Cell Metabolism and Diseases, State Key Laboratory of Conservation and Utilization of Bio-resources in Yunnan Center for Life Sciences, School of Life Sciences, Yunnan University, China

#These authors contributed equally: Yating Liu[#], Guojing Tian[#]

* Corresponding Author：Zhao Shan (shanzhaolab@163.com) , Bin Qi (qb@yun.edu.cn)

Lead Contact: Bin Qi, Email: qb@ynu.edu.cn

Summary

The ability to sense and adapt to adverse food conditions is essential for survival across species, but the detailed mechanisms of neuron-digestive crosstalk in food sensing and adaptation remain poorly understood. This study identifies a novel mechanism by which animals detect unfavorable food sources through olfactory neurons and initiate a systemic response to shut down digestion, thus safeguarding against potential harm. Specifically, we demonstrate that NSY-1, expressed in AWC olfactory neurons, detects *Staphylococcus saprophyticus* (SS) as an unfavorable food source, prompting the animal to avoid and halt digestion of SS. Upon detection, the animals activate the AWC^{OFF} neural circuit, leading to a systemic digestive shutdown, which is mediated by NSY-1-dependent STR-130. Additionally, NSY-1 mutation triggers the production of insulin peptides, including INS-23, which interact with the DAF-2 receptor to modulate SS digestion and affects the expression of intestinal BCF-1. These findings uncover a crucial survival strategy through neuron-digestive crosstalk, where the NSY-1 pathway in AWC neurons orchestrates food evaluation and initiates digestive shutdown to adapt effectively to harmful food sources.

Key words: Digestion, AWC neuron, NSY-1, Food behavior, *C. elegans*

Introduction

Food is a source of essential nutrients and also poses a risk of lethal toxins and pathogens. Animals, including humans, must respond to various food sources to ensure survival. The ability to detect and adapt to adverse food conditions is crucial for the survival of many species. Various sensory mechanisms have evolved to monitor food quality by detecting beneficial and harmful substances, include olfactory (Fiala, 2007; McLachlan et al., 2022; Sengupta et al., 1996), gustatory (Avery et al., 2021; Hukema et al., 2006; Scott, 2018), and gut chemosensory systems (Bargmann, 2006). Food allergies serve as a biological food quality control system, offering protection and benefits by promoting food avoidance behavior (Florsheim et al., 2021). Research by Plum et al. (Plum et al., 2023) and Florsheim et al. (Florsheim et al., 2023) provides evidence that the immune system's allergic response communicates with the brain in mice, leading to food avoidance. This avoidance behavior acts as a defense strategy, reducing the risk of exposure to harmful substances, including allergens.

The digestive system functions by transporting food through the gastrointestinal (GI) tract, where it is broken down into molecules that can be absorbed and utilized by the body's cells. Thus, shutdown of digestion may serve as a mechanism for eliminating indigestible or harmful substances, acting as a protective system in animals to avoid adverse food. Despite this, the interaction between neuronal food detection and intestinal digestion, particularly in assessing and adapting to harmful food, remains inadequately understood.

The free-living nematode *Caenorhabditis elegans* thrives in organic-rich environments where it encounters a variety of microorganisms as food (Felix and Braendle, 2010; Samuel et al., 2016; Schulenburg and Felix, 2017). *C. elegans* has evolved mechanisms to sense bacterial presence and food quality, which influence its feeding behaviors and digestive processes to adapt to its environment. Previous research has identified heat-killed *E. coli* as low-quality food, which the nematode avoids using its food-quality evaluation systems, such as the FAD-ATP-TORC1-ELT-2 pathway (Qi et al., 2017) and the UPR^{ER}–immunity pathway (Liu et al., 2024). Additionally, we have found that certain bacteria, like

Staphylococcus saprophyticus (SS), are classified as inedible, leading to shutting down digestion and stunted growth in the nematodes (Geng et al., 2022). However, we still need to determine whether SS represents harmful food for *C. elegans* and how the nematode senses SS and shuts down digestion to reject it. It is hypothesized that *C. elegans* may detect or assess inedible food, such as SS, and subsequently halt digestion as a survival strategy. This suggests that the cooperation between food sensing and digestive systems could form a systemic food quality control mechanism in animals, aimed at minimizing the adverse effects of harmful food.

In this study, we developed a model in *C. elegans* to investigate responses to harmful food and explored how the nematodes sense and avoid ingesting such food by shutting down their digestive systems. We identified a food quality control mechanism involving communication between neurons and the digestive system. This mechanism functions as a defense strategy to minimize the adverse effects of harmful food environments on the animals.

Results

Shutting Down Digestion as a Protective Mechanism for Survival in Larval *C. elegans*

Previous studies have shown that *Caenorhabditis elegans* cannot digest *Staphylococcus saprophyticus* (SS), which prevents their development (Figure 1A). In natural environments, *C. elegans* rely on various bacteria for nutrition and growth. However, SS is not a viable food source for *C. elegans*. Larval arrest, such as the dauer stage, serves as an adaptive mechanism for survival under unfavorable conditions, including limited food availability or extreme temperatures. We hypothesize that *C. elegans* can sense or evaluate inedible food, such as SS, and subsequently shut down their digestion to arrest development as a protective survival strategy (Figure 1B).

Our previous research demonstrated that *C. elegans* can assess and avoid low-quality food, like heat-killed *E. coli*, to adapt to nutrient-deficient conditions (Liu et al., 2024; Qi et al., 2017). To determine if *C. elegans* also detect SS as an unfavorable food source, we conducted two behavioral assays: food dwelling/avoidance and food

choice (Qi et al., 2017). In the food dwelling/avoidance assay, larval-stage animals exhibited strong discrimination against SS compared to the standard food, OP50 (Figure 1C). In the food choice assay, the animals preferred OP50 over low-quality food such as heat-killed *E. coli* (Figure S1A) or SS (Figure 1D). However, they could not distinguish between heat-killed *E. coli* and SS (Figure S1B). These results suggest that SS acts as an unfavorable food that *C. elegans* can detect and avoid.

In response to starvation, L1 larvae can enter a state of developmental arrest, pausing their growth to survive (Baugh and Sternberg, 2006). To test whether *C. elegans* shut down digestion of SS as a protective strategy upon sensing unfavorable food, we performed a survival assay on L1 larvae fed with SS. We found that larvae unable to digest SS still survived under SS feeding conditions (Figure S1C), similar to larvae under L1 starvation. This suggests that shutting down digestion may be a protective mechanism in larvae under SS feeding conditions.

Previously, we observed that activating larval digestion with heat-killed *E. coli* or *E. coli* cell wall peptidoglycan (PGN) enabled the digestion of SS as food (Hao et al., 2024). Additionally, when animals reached the L2 stage on a normal OP50 diet, they could utilize SS as a food source to support growth (Figure S1D). These findings suggest that once the digestive system is activated, *C. elegans* no longer detect SS as unfavorable, leading to digestion. If SS is indeed an unfavorable or toxic food for *C. elegans*, digesting it could result in physiological defects. We measured the lifespan of L4 stage animals fed with SS or OP50. We found that SS consumption shortened their lifespan (Figure 1E-F), indicating a cost associated with digesting unfavorable or toxic food.

In conclusion, our data suggest that larval-stage *C. elegans* can sense and evaluate SS as an unfavorable food source, leading to the shutdown of digestion to avoid consumption, thereby protecting them and allowing adaptation to an unfavorable food environment.

C. elegans **Sense SS and Shut Down Digestion through NSY-1**

We speculated that key factors in *C. elegans* are involved in sensing *Staphylococcus saprophyticus* (SS) and shutting down its digestion. If these factors are mutated, the animals would fail to detect SS as an unfavorable food source and would utilize it

(Figure S2A). To identify these factors, we conducted an unbiased forward genetic screen to find mutant animals that cannot sense SS, thereby allowing its digestion and supporting growth. One of the mutant alleles identified, *ylf6*, could digest SS and exhibited a growth phenotype under SS feeding conditions (Figure S2B). Whole-genome deep sequencing revealed that *ylf6* carries two mutations in the *nsy-1* gene (H929Y, Q1191*) (Figure S2C).

To confirm that *nsy-1* is essential for shutting down SS digestion, we used an independent *nsy-1* mutant allele, *ag3*, and found that *nsy-1(ag3)* mutants also digested SS (Figure 2A). To determine whether *nsy-1* is crucial for sensing SS, we performed two behavioral assays: food dwelling/avoidance and food choice. In the food dwelling/avoidance assay, larval stage *nsy-1* mutant animals showed reduced discrimination against SS compared to wild-type N2 animals (Figure 2B). In contrast to wild-type N2 animals, *nsy-1* mutants preferred SS when given a choice between two poor-quality foods, heat-killed *E. coli* and SS (Figure 2C, Figure S1B). These results suggest that *nsy-1* is essential for *C. elegans* to sense and avoid SS.

Next, we examined whether larvae that cannot sense SS and do not shut down digestion can adapt to SS environments. We measured the survival rate of *nsy-1* mutants under SS feeding conditions and found that these mutants had a higher mortality rate (Figure 2D).

Overall, these results indicate that *C. elegans* sense and detect unfavorable food, such as SS, through *nsy-1*, and subsequently shut down digestion to protect themselves and enhance survival.

NSY-1 Functions in AWC Neurons to Shut Down SS Digestion

The *nsy-1* gene in *C. elegans* encodes a MAP kinase kinase kinase (MAPKKK) that operates in the AWC neurons (Kim et al., 2002; Sagasti et al., 2001), which are essential for chemotaxis and odor sensation. The primary role of *nsy-1* in AWC neurons is to regulate the asymmetric expression of odorant receptors, contributing to neuronal asymmetry and diversity (Chuang et al., 2007; Sagasti et al., 2001). We hypothesized that the shutdown of SS digestion in *C. elegans* is mediated by *nsy-1* function in AWC neurons.

Firstly, we constructed a P*nsy-1*::GFP reporter strain and confirmed that *nsy-1* is expressed in the AWC neurons (Figure 3A). Secondly, we expressed *nsy-1* in the AWC neurons of *nsy-1* mutant animals and observed that the transgenic animals rescued the indigestion phenotype (Figure 3B). This indicates that *nsy-1* functions in AWC neurons to shut down SS digestion. Thirdly, we used CRISPR to construct a mutant strain that knocks out *nsy-1* specifically in AWC neurons (Figure S3). We found that *nsy-1* knockout in AWC neurons also resulted in the shutdown of SS digestion (Figure 3C).

These results collectively suggest that NSY-1 is functional in AWC neurons and is crucial for shutting down SS digestion in *C. elegans*.

AWC Neurons Exhibit OFF State in Sensing SS Food

In *C. elegans*, the expression of the *str-2* gene in AWC neurons indicates the ON state (AWC^{ON}) (Sagasti et al., 2001), which is associated with high cGMP levels and lower calcium activity, enabling the neuron to respond to specific odors. Conversely, the absence of *str-2* expression marks the OFF state (AWC^{OFF}), characterized by different odor responses, low cGMP levels, and higher calcium activity (Troemel et al., 1999). We aimed to investigate (1) whether AWC neurons exhibit different states under normal food (*E. coli* OP50) versus unfavorable food (SS) conditions and (2) whether the state of AWC neurons affects the ability of *C. elegans* to digest SS.

Using *str-2*::GFP as a marker for AWC neuron states (Troemel et al., 1999), we found that wild-type animals feeding on normal OP50 food typically exhibit one AWC^{OFF} and one AWC^{ON} neuron. However, when feeding on SS, the proportion of animals with the AWC^{OFF} state increased, with approximately 50% of animals exhibiting two AWC^{OFF} neurons (Figure 3D, E, F).

In *nsy-1* mutant animals feeding on OP50, *str-2*::GFP is expressed in both AWC neurons ($2AWC^{ON}$), consistent with previous studies (Chuang and Bargmann, 2005; Chuang et al., 2007; Sagasti et al., 2001; Troemel et al., 1999) (Figure 3D, E). Notably, both AWC neurons remained in the AWC^{ON} state in *nsy-1* mutants feeding on SS (Figure 3D, E). These results suggest that SS feeding induces an AWC^{OFF} state in wild-type animals, while the *nsy-1* mutation promotes an AWC^{ON} state even under

SS feeding conditions. This implies that the AWC^{OFF} state may inhibit SS digestion, whereas the AWC^{ON} state promotes it.

The TIR-1-NSY-1-SEK-1-MAPK pathway plays a crucial role in regulating the asymmetric AWC cell fate decision. Previous studies have shown that *str-2*::GFP expression in both AWC cells ($2AWC^{ON}$ phenotype) occurs in *tir-1*, *nsy-1*, and *sek-1* mutant animals (Chuang and Bargmann, 2005; Sagasti et al., 2001; Troemel et al., 1999). We found that *tir-1* mutant can grow under SS feeding conditions (Figure 3G), indicating that *tir-1* mutant can digest SS similarly to *nsy-1* mutants. This demonstrates that the AWC^{ON} state promotes SS digestion.

Overall, our data suggest that the state of AWC neurons is critical for sensing food in *C. elegans*. When sensing SS food, animals exhibit an AWC^{OFF} state, which shuts down digestion. Conversely, the AWC^{ON} state promotes the digestion of SS.

NSY-1 Shuts Down SS Digestion through Induction of STR-130

We have demonstrated that NSY-1 in AWC neurons detects unfavorable food and shuts down digestion (Figure 3). To investigate the genes regulated by NSY-1 in response to SS and their impact on SS digestion, we conducted a transcriptomic analysis on L1 larval animals fed with normal food (OP50) or unfavorable food (SS) for a short duration (4 hours). We speculated that some genes induced by SS food are dependent on NSY-1 (Figure 4A), and their induction aids in shutting down SS digestion.

RNA-seq data analysis revealed 304 NSY-1-dependent candidate genes responding to SS (Figure 4B, Table S1). Enrichment analysis (Figure S4A, Table S2) of these candidate genes showed mainly associations with biotic stimulus, defense responses, xenobiotic stimulus, suggesting that NSY-1 positively regulates stress response pathways to protect animals under harmful food, SS, feeding conditions. Moreover, we found that sensory perception related genes (*sra-32, str-87, str-112, str-130, str-160, str-230*) (Figure S4A, Table S2) were also enriched, with many genes being G protein-coupled receptors (GPCRs), which mediate odor sensing (Buck and Axel, 1991). Our study indicated that wild-type *C. elegans* respond to SS by regulating olfactory AWC neurons (Figure 3D, E), potentially influenced by GPCRs. We further analyzed the dependence of these enriched GPCRs on NSY-1 under SS feeding

conditions (Figure S4B) and found that *str-130* is significantly upregulated in response to SS, with its function strong being NSY-1 dependent (Figure 4C).

It has been shown that *str-130* is expressed in AWC^{OFF} neurons, based on transgenic GFP reporter strains, *str-130p*::GFP (Vidal et al., 2018). Our data also show that *str-130* expression is induced in wild-type animals fed with SS (Figure 4C), where AWC neurons exhibit the AWC^{OFF} state (Figure 3D, E). Therefore, it is possible that the high expression of *str-130*, regulated by *nsy-1*, alters the AWC state and inhibits SS digestion.

Firstly, we found that knockdown of *str-130* in wild-type animals promoted SS digestion, thereby supporting animal growth (Figure 4D), and the proportion of animals with two AWC^{OFF} neurons decreased (Figure 4E). Secondly, we found that overexpression of *str-130* in *nsy-1* mutant animals inhibited SS digestion, thereby slowing animal growth (Figure 4F), and the proportion of animals with two AWC^{OFF} neurons increased (Figure 4G). These results demonstrate that NSY-1 promotes the AWC^{OFF} state by inducing *str-130* expression, which in turn inhibits SS digestion in *C. elegans*.

NSY-1 Mutation Promotes SS Digestion by Inducing Insulin Signaling

NSY-1 mutation promotes the digestion of unfavorable food, such as SS, and supports *C. elegans* growth (Figure 2A). We hypothesize that, in addition to upregulating certain genes, such as *str-130*, to inhibit SS digestion, NSY-1 may also suppress certain genes to prevent nematodes from utilizing SS (Figure 5A). One possibility is that some genes, induced by the *nsy-1* mutation under SS feeding conditions could facilitate SS digestion in the *nsy-1* mutant (Figure 5A).

Our RNA-seq analysis identified 308+46=354 genes that are induced by the *nsy-1* mutation under SS feeding conditions (Figure 5B, Table S3). However, among these 354 genes, 46 genes can also be induced in wild-type animals fed with SS, suggesting that these 46 genes may not be involved in digesting SS in *nsy-1* mutants. Therefore, the 308 candidate genes induced by the *nsy-1* mutation under SS feeding conditions could potentially promote animals to digest SS.

Enrichment analysis revealed that genes related to extracellular functions, such as insulin-related genes, are induced in *nsy-1* mutant animals (Figure S5A, Table S4).

Further analysis of insulin-related genes from the RNA-seq data showed that *ins-23* is predominantly induced in *nsy-1* mutant animals (Figure S5B), suggesting its potential role in promoting SS digestion. We found that knockdown of *ins-23* in *nsy-1* mutants inhibited SS digestion (Figure 5D). These results demonstrate that the *nsy-1* mutation induces the insulin peptide *ins-23*, which promotes SS digestion.

The insulin/insulin-like growth factor signaling (IIS) pathway, particularly through the DAF-2 receptor, integrates nutritional signals to regulate various behavioral and physiological responses related to food (Kodama et al., 2006; Ryu et al., 2018). It has been shown that INS-23 acts as an antagonist for the DAF-2 receptor to promote larval diapause (Matsunaga et al., 2018). To test whether *ins-23* induction in *nsy-1* mutants promotes SS digestion through its receptor, DAF-2, we constructed a *nsy-1; daf-2* double mutant. We found that the SS digestion ability of the *nsy-1* mutant was inhibited by the *daf-2* mutation. This suggests that the *nsy-1* mutation induces the insulin peptide *ins-23*, which promotes SS digestion through its potential receptor, DAF-2.

NSY-1 Mutation Promotes SS Digestion through Regulation of Intestinal BCF-1

In our previous study, we found that heat-killed *E. coli* promotes SS digestion in *C. elegans* (Geng et al., 2022), a process requiring intestinal BCF-1 (Hao et al., 2024). In the absence of BCF-1, the digestive capability of the animals is significantly reduced (Hao et al., 2024). This led us to investigate whether NSY-1 in AWC neurons regulates intestinal *bcf-1* expression.

Firstly, we used a *bcf-1*::GFP reporter to measure *bcf-1* expression in *nsy-1* mutant animals. We found that mutation of *nsy-1* induced *bcf-1* expression in animals fed either SS or OP50 food (Figure 6A). Additionally, we confirmed that *nsy-1* mutation in AWC neurons also induced intestinal *bcf-1* expression under SS feeding conditions (Figure 6B). This data indicates that NSY-1 in AWC neurons inhibits intestinal *bcf-1* expression, implying that *nsy-1* mutation promotes SS digestion through BCF-1.

Next, we constructed a *nsy-1; bcf-1* double mutant and analyzed the growth of these animals on SS. We found that the digestive ability of *nsy-1* mutants was inhibited by the mutation of *bcf-1* (Figure 6C). Together, our data suggest that the increased

digestion ability in *nsy-1* mutant animals is dependent on the intestinal digestion factor BCF-1.

We then asked how *nsy-1* regulates intestinal *bcf-1* expression. Since *nsy-1* mutation induces the insulin peptide *ins-23*, which promotes SS digestion, we tested whether the induction of intestinal *bcf-1* by *nsy-1* mutation is also mediated through INS-23. We found that the *bcf-1*::GFP level decreased in *nsy-1* mutant animals following *ins-23* RNAi treatment (Figure 6D). This suggests that *nsy-1* mutation activates *bcf-1* expression in the intestine, which requires INS-23.

It has been reported that DAF-2 acts as the receptor for INS-23 (Matsunaga et al., 2018). Therefore, we also investigated whether INS-23-induced digestion in *nsy-1(ag3)* is mediated through its receptor, DAF-2. Our findings revealed that the food digestion phenotype of *nsy-1(ag3)* was impaired by mutations in *daf-2* (Figure 6E), indicating that the enhanced digestion observed in *nsy-1(ag3)* mutants also relies on INS-23's receptor, DAF-2.

Overall, our data indicated that *nsy-1* mutation promotes SS digestion through inducing intestinal *bcf-1*, which is regulated by INS-23.

Discussion

This study in *Caenorhabditis elegan*s reveals a neural-digestive mechanism for evaluating harmful food (Figure 7). The olfactory neuron-expressed NSY-1 protein detects *Staphylococcus saprophyticus* (SS) as unsafe food, triggering a digestive shutdown via the AWC^{OFF} neural circuit and the NSY-1-dependent STR-130. Mutations in NSY-1 lead to SS digestion, activating the insulin/IGF-1 signaling (IIS) pathway and BCF-1 expression. These findings highlight a food quality evaluation strategy where neurons communicate with the digestive system to assess food safety, providing insights into how animals adapt to toxic food environments.

The identification of NSY-1 in AWC olfactory neurons as a key player in detecting *Staphylococcus saprophyticus* (SS) and initiating digestive shutdown is particularly intriguing. NSY-1, a MAP kinase (MAPKKK), is known to regulate the asymmetric expression of odorant receptors, contributing to neuronal asymmetry and diversity

(Chuang and Bargmann, 2005; Chuang et al., 2007; Sagasti et al., 2001; Troemel et al., 1999). Previous research has demonstrated that AWC neurons are pivotal in chemotaxis and sensory processing (Bargmann et al., 1993; Troemel et al., 1997; Wes and Bargmann, 2001) . Our findings extend its function to include food quality assessment, showing that NSY-1 can trigger a digestive shutdown via the AWC^{OFF} neural circuit. This highlights a sophisticated system where olfactory inputs directly influence digestive processes. It suggests that the olfactory system, beyond its primary function of detecting odors, may also play a significant role in monitoring food quality and signaling the digestive system.

This neural circuit appears to be a crucial component of a systemic food quality control mechanism, allowing animals to adapt effectively to harmful food sources. The state of AWC neurons (AWC^{ON} or AWC^{OFF}) directly influences the animal's ability to digest SS, with the AWC^{OFF} state inhibiting digestion and the AWC^{ON} state promoting it. The finding that activation of the AWC^{OFF} neural circuit leads to a systemic digestive shutdown mediated by NSY-1-dependent GPCR(STR-130) is another notable advancement. GPCRs are well-known for their roles in sensory perception (Julius and Nathans, 2012; Troemel et al., 1995). Our results suggested that GPCR STR-130 play a role in shutting down digestive processes though maintaining AWC^{OFF} states for evaluating harmful food.

Our study underscores the critical role of insulin signaling pathways in mediating the effects of neuronal detection on intestinal functions. Upon detection of SS by AWC neurons, NSY-1 inhibits the expression of insulin-like peptides, particularly INS-23. These peptides interact with the DAF-2 receptor in the gut, influencing the expression of BCF-1, a key regulatory factor in digestion (Hao et al., 2024). Once ins-23 was inhibited by neuronal NSY-1, the intestinal BCF-1 level is also reduced, which in turn shutdown digestion. We found that the digestive ability of *nsy-1* mutants was totally inhibited by the mutation of *bcf-1* (Figure 6C), suggest that the increased digestion ability in *nsy-1* mutant animals is mainly dependent on the intestinal digestion factor BCF-1. This regulatory cascade highlights the intricate link between neuronal signals and gut responses, ensuring an adaptive reaction to harmful food. We speculated that except INS-23, there should be other factors as signaling regulated by neuronal NSY-1 to inhibits intestinal digestion factor BCF-1 for digestion shutdown.

Future studies should focus on delineating the precise molecular pathways linking NSY-1 signaling in AWC neurons to digestion regulation in the gut. Identifying the role of other sensory neurons in food quality assessment and their interactions with

the digestive system may uncover new facets of neuron-gut communication and adaptive responses.

In summary, our study reveals a sophisticated mechanism in *C. elegans* that integrates neuronal detection of harmful food sources with systemic digestive responses. This neuron-digestive crosstalk is crucial for maintaining organismal homeostasis and survival in the presence of toxic food sources. The findings suggest that similar pathways may exist in other species, including humans, providing a foundation for future research on food safety, toxin avoidance, and the neural regulation of digestive processes. This has important implications for public health, as it illuminates the biological mechanisms underlying foodborne illness and the body's defenses against such threats.

Author Contributions

Y. L and G.T performed experiments, analyzed data and wrote the paper; Z. W performed phenotype analysis; J. Z performed EMS screen; H. L analyzed EMS sequencing data; S. Z supervised some experiments; Z. S supervised some experiments, wrote and revised this paper; B.Q. supervised this study, and wrote the paper with inputs from G. T and Y. L.

Acknowledgments

We thank the Caenorhabditis Genetics Center (CGC) (funded by NIH P40OD010440) for strains; We thank Dr. Huanhu Zhu and Dr. Xiajing Tong (ShanghaiTech University), Dr. Hongyun Tang (Westlake University), Dr. Zhiyong Shao (Fudan University) for sharing strains. This work was supported by the Ministry of Science and Technology of the People’s Republic of China (2019YFA0803100，2019YFA0802100 to B.Q), the National Natural Science Foundation of China (32071129 to Z.S., 32170794 to B.Q.), Yunnan Provincial Science and Technology Project at Southwest United Graduate School (202302AP370005 to B.Q.), Yunnan Applied Basic Research Projects (202201AT070196 to B.Q.), Yunnan Revitalization Talent Support Program (C619300A086 to Z.S., K264202230211 to B.Q.).

Declaration of interests

The authors declare no competing interests.

Main Figure Legends:

Figure 1. *C. elegans* shuts down its digestion for survival when fed harmful food, specifically *Staphylococcus saprophyticus* (SS).

(A) Microscopic images showing worms fed with SS arrested at the L1 stage three days after hatching.

(B) Schematic model illustrating our hypothesis: *C. elegans* can sense or evaluate inedible food, such as SS, and subsequently shut down their digestion to arrest development as a protective survival strategy.

(C) Schematic drawing and quantitative data of the food dwelling/avoidance assay. Yellow circles indicate the food spot for OP50 or SS bacteria, respectively. The animals were scored at the indicated times after L1 worms were placed on the food spot. The red point indicates the position of each worm. Data are represented as mean ± SD. Bar = 1000 μm. ***$p < 0.001$; **$p < 0.01$ by Student's t-test.

(D) Schematic drawing, microscopic images, and quantitative data of the food choice assay. L1 worms were placed at the center spot (origin). OP50 (yellow) and SS (blue) bacteria were placed on opposite sides of the plate. The red point indicates the position of each worm. The percentage of worms on each spot was calculated at the indicated times. Data are represented as mean ± SD. Bar = 1000 μm. ****$p < 0.0001$; **$p < 0.01$ by Student's t-test.

(E-F) Schematic drawing and quantitative data of the lifespan of animals fed with SS or OP50. L1 worms were seeded onto OP50 and grown to the L4 stage. L4 worms were then moved to SS or OP50 food to measure lifespan. **$p < 0.01$ by log-rank test. All data are representative of at least three independent experiments.

Figure 2. *C. elegans* senses SS and shuts down digestion through NSY-1.

(A) Developmental phenotype of wild-type N2 and *nsy-1(ag3)* mutant worms fed with SS bacteria. Data are represented as mean ± SD. Bar = 200 μm.. ****$p < 0.0001$ by Student's t-test.

(B) Schematic drawing, microscopic images, and quantitative data of the food dwelling/avoidance assay. Yellow circles indicate the food spot for SS bacteria. The animals were scored 4 hours after L1 worms were placed on the food spot. The blue circle indicates the edge of the bacterial lawn, and the red point indicates the position of each worm. Data are represented as mean ± SD. Bar = 1000 μm. **$p < 0.01$ by Student's t-test.

(C) Schematic drawing, microscopic images, and quantitative data of the food choice assay. L1 *nsy-1(ag3)* worms were placed at the center spot (origin). Heat-killed OP50

(yellow) and SS (blue) bacteria were placed on opposite sides of the plate. The red point indicates the position of each worm. The percentage of worms on each spot was calculated at the indicated times. Data are represented as mean ± SD. Bar = 1000 μm. **p < 0.01; ***p < 0.001 by Student's t-test.

(D) Survival curves of wild-type N2 and *nsy-1(ag3)* mutant worms fed with SS bacteria. L4 worms, previously fed OP50 bacteria, were transferred to SS food to measure lifespan. ****p < 0.0001 by log-rank test.

All data are representative of at least three independent experiments.

Figure 3. NSY-1 plays a critical role in AWC neurons to inhibit SS digestion.

(A) Microscopic image showing the expression pattern of *nsy-1*. The head of an adult transgenic animal carrying *Pnsy-1::GFP* and *Podr-1::RFP* shows colocalization of *nsy-1* and *odr-1*. Bar = 20 μm.

(B) Developmental progression of *nsy-1(ag3)* mutant worms carrying *Podr-1::nsy-1::gfp* (AWC neuron-specific expression) grown on SS bacteria. Control animals are labeled with white stars, and animals carrying the transgenes (rescued animals) are labeled with yellow stars. Data are represented as mean ± SD. Bar = 200 μm. ****p < 0.0001 by Student's t-test.

(C) Developmental progression of wild-type N2 and AWC neuron-specific knockout *nsy-1* animals (AWC *nsy-1* KO) grown on SS bacteria. Data are represented as mean ± SD. Bar = 500 μm. ***p < 0.001 by Student's t-test.

(D) Microscopic images show *str-2::GFP*, a marker for AWC neuron states, in L1-staged wild-type and *nsy-1(ky397)* mutant worms grown on OP50 or SS bacteria for 6 hours. AWC neuron positions are highlighted with red and yellow arrows. Bar = 20 μm.

(E-F) Percentage of animals with different AWC neuron states. *nsy-1* mutation promotes an $2AWC^{ON}$ state under SS feeding conditions (E), with approximately 50% of animals exhibiting $2AWC^{OFF}$ neurons when feeding on SS (F). Data are represented as mean ± SD. ****p < 0.0001 by Student's t-test.

(G) Developmental progression of wild-type N2, *tir-1(qd4)*, and *nsy-1(ag3)* mutant worms grown on SS bacteria. Data are represented as mean ± SD. Bar = 200 μm. ****p < 0.0001 by Student's t-test.

All data are representative of at least three independent experiments.

Figure 4. NSY-1 inhibits animals from digesting SS by inducing *str-130*.

(A) Schematic illustration showing that "X" genes rely on NSY-1 to shut down SS

digestion. "X" genes induced by SS food are dependent on NSY-1, and their induction aids in shutting down SS digestion.

(B) Venn diagram showing the overlap of genes that respond to SS and rely on NSY-1. The number of genes is indicated in the diagram (also see Table S1).

(C) Transcriptome analysis showing *str-130* mRNA expression, which relies on NSY-1 in response to SS. Data are represented as mean ± SD. ****p < 0.0001; **p < 0.01; *p < 0.05 by Student's t-test.

(D) Developmental progression of wild-type animals treated with control RNAi or *str-130* RNAi grown on SS bacteria. Data are represented as mean ± SD. Bar = 200 μm. ****p < 0.0001 by Student's t-test.

(E) Microscopic images and quantitative data of AWC neuron states in L1 animals treated with control RNAi or *str-130* RNAi grown on SS bacteria. Data are represented as mean ± SD. Bar = 20 μm. ***p < 0.001 by Student's t-test ($1AWC^{ON}/1AWC^{OFF}$: control vs *str-130* RNAi).

(F) Developmental progression of *nsy-1(ag3)* mutant worms carrying *Pstr-130::str-130::mCherry* grown on SS bacteria. Control animals are labeled with white stars, and animals carrying transgenes are labeled with yellow stars. Data are represented as mean ± SD. Bar = 400 μm. ***p < 0.001 by Student's t-test.

(G) Microscopic images and quantitative data of AWC neuron states in L1 animals carrying *Pstr-130::str-130::mCherry*. Transgenic animals with overexpression of *str-130* (carrying *Pord-1::GFP* as a co-injection marker) show an increased $2AWC^{OFF}$ state. Data are represented as mean ± SD. Bar = 20 μm. ****p < 0.001 by Student's t-test ($2AWC^{OFF}$: Control vs Transgene).

All data are representative of at least three independent experiments.

Figure 5. NSY-1 mutation activates animals to digest SS by inducing insulin signaling.

(A) Schematic illustration showing that NSY-1 inhibits the expression of "Y" genes, which promote SS digestion. Some genes induced by the *nsy-1* mutation under SS feeding conditions could facilitate SS digestion in the *nsy-1* mutant.

(B) Venn diagram showing the overlap of genes that respond to SS but are limited by NSY-1. A total of 308 candidate genes induced by the *nsy-1* mutation under SS feeding conditions could potentially promote SS digestion.

(C) Transcriptome analysis showing that *ins-23* expression is induced in animals with the *nsy-1* mutation under SS feeding conditions. Data are represented as mean ± SD. **p < 0.01; n.s. not significant by Student's t-test.

(D) Developmental progression of *nsy-1(ag3)* mutant animals treated with control

RNAi or *ins-23* RNAi grown on SS bacteria. Data are represented as mean ± SD. Bar = 500 μm. ****p < 0.0001 by Student's t-test.

(E) Developmental progression of *nsy-1(ag3), daf-2(e1370),* and *nsy-1(ag3);daf-2(e1370)* double mutant animals grown on SS bacteria. Data are represented as mean ± SD. Bar = 500 μm. ****p < 0.0001 by Student's t-test.

All data are representative of at least three independent experiments.

Figure 6. NSY-1 mutation promotes animals to digest SS through inducing intestinal *bcf-1*.

(A) Microscopic images and quantitative data showing fluorescence of *Pbcf-1::bcf-1::GFP* in L1-staged wild-type (WT) and *nsy-1(ag3)* mutant animals fed with OP50 or SS bacteria for 6 hours. Data are represented as mean ± SD. Bar = 100 μm. ****p < 0.0001 by Student's t-test.

(B) Microscopic images and quantitative data showing fluorescence of *Pbcf-1::bcf-1::GFP* in L1-staged wild-type and AWC *nsy-1* KO mutant (AWC neuron-specific knockout *nsy-1* animals) fed with SS bacteria for 6 hours. Data are represented as mean ± SD. Bar = 50 μm. ***p < 0.001 by Student's t-test.

(C) Developmental progression of wild-type N2, *nsy-1(ag3), bcf-1(ok2599),* and *nsy-1(ag3);bcf-1(ok2599)* double mutant animals grown on SS bacteria. Data are represented as mean ± SD. Bar = 200 μm. ****p < 0.0001; n.s. not significant by Student's t-test.

(D) Microscopic images and quantitative data showing fluorescence of *Pbcf-1::bcf-1::GFP* in *nsy-1(ag3)* mutant animals treated with control RNAi or *ins-23* RNAi under normal RNAi feeding conditions. Data are represented as mean ± SD. Bar = 200 μm. ****p < 0.0001 by Student's t-test.

All data are representative of at least three independent experiments.

Figure 7. A model reveals a neural-digestive mechanism for evaluating harmful food.

(A) AWC neuron-expressed NSY-1 detects *Staphylococcus saprophyticus* (SS) as harmful food and shuts down digestion by inducing the AWC^{OFF} neural circuit and NSY-1-dependent STR-130. This mechanism protects the animals and helps them avoid harmful food.

(B) Mutations in NSY-1 lead to SS digestion by activating the insulin/IGF-1 signaling (IIS) pathway and BCF-1 expression, thereby reducing the animals' ability to avoid harmful food and decreasing their protection.

Supplemental Figure Legends:

Figure S1. SS is harmful food that animals cannot digest. Related to Figure 1.
(A) Schematic drawing, microscopic images, and quantitative data from the food choice assay. L1 worms were placed at the center spot (origin). OP50 (yellow) and heat-killed OP50 (blue) bacteria were positioned on opposite sides of the plate. The red point indicates the position of each worm. The percentage of worms on each spot was calculated at the indicated times. Data are represented as mean ± SD. Bar = 1000 μm. ****$p < 0.0001$; ***$p < 0.001$; **$p < 0.01$ by Student's t-test.
(B) Schematic drawing, microscopic images, and quantitative data from the food choice assay. L1 worms were placed at the center spot (origin). Heat-killed OP50 (blue) and SS (red) bacteria were positioned on opposite sides of the plate. The red point indicates the position of each worm. The percentage of worms on each spot was calculated at the indicated times. Data are represented as mean ± SD. Bar = 1000 μm. ****$p < 0.0001$; n.s. not significant by Student's t-test.
(C) Schematic drawing and quantitative data of the lifespan of animals fed with SS or OP50. L1 worms were seeded on plates with no food (NGM) or SS bacteria to measure lifespan. n.s. not significant by log-rank test.
(D) Schematic drawing and quantitative data of the developmental progression of wild-type N2 under different feeding conditions. L1 animals were seeded onto OP50 plates and grown to the L2 stage. L2 animals were then transferred to OP50, SS, or no food (NGM) plates to measure worm length at the indicated time points.
All data are representative of at least three independent experiments.

Figure S2. EMS screen to identify genes involved in shutting down digestion of SS. Related to Figure 2.
(A) Schematic illustration of the EMS screen strategy to identify "Y" genes involved in shutting down digestion after sensing SS. In mutants with defects in "Y" genes, digestion of SS is restored, allowing the mutants to grow on SS.
(B) Developmental phenotype of wild-type N2 and *ylf6* mutant worms fed with SS bacteria. Bar = 200 μm.
(C) Schematic drawing showing the mutation sites in *nsy-1(ylf6)* and *nsy-1(ag3)*.

Figure S3. Construction of *nsy-1* specific knockout in AWC neurons using CRISPR-Cas9. Related to Figure 3.

Representative DNA gels showing NheI digestion of PCR-amplified genomic DNA extracted from wild-type (WT) worms and worms with *nsy-1*-specific knockout in AWC neurons (*odr-1p::Cas9* + *u6p::nsy-1-sg*).

Figure S4. *str-130* is induced in wild-type in response to SS, dependent on NSY-1.
(A) GO enrichment analysis of 304 NSY-1-dependent candidate genes responding to SS (Figure 4B, Table S2). Genes related to sensory perception (*sra-32, str-87, str-112, str-130, str-160, str-230*) are highlighted as enriched (red arrow).
(B) Relative mRNA expression levels of sensory perception-related genes (*sra-32, str-87, str-112, str-130, str-160, str-230*) extracted from RNA-seq data. These genes are induced in wild-type N2 animals in response to SS, but their expression is reduced in *nsy-1(ag3)* mutant animals under SS feeding conditions, indicating that the induction of these genes in wild-type in response to SS is dependent on NSY-1.

Figure S5. *nsy-1* mutation induces the expression of insulin-related genes. Related to Figure 5.
(A) GO enrichment analysis of 308 genes induced by the nsy-1 mutation under SS feeding conditions (Figure 5B, Table S2).
(B) Relative mRNA expression levels of insulin-related genes (*ins-23, ins-22, ins-27, ins-24*) extracted from RNA-seq data. These genes are upregulated in *nsy-1(ag3)* mutant animals under SS feeding conditions, which may contribute to SS digestion in the *nsy-1* mutant.

Supplemental Table Legends:

Table S1. List of genes induced by SS food that are dependent on NSY-1. Related to Figure 4B.
Table S2. GO enrichment analysis of 304 NSY-1-dependent candidate genes responding to SS. Related to Figure S4A and 4B.
Table S3. List of genes induced in *nsy-1(ag3)* mutant animals feeding on SS. Related to Figure 5B.
Table S4. GO enrichment analysis of 308 genes induced by the nsy-1 mutation under SS feeding conditions. Related to Figure S5A and 5B.

Star Methods

Resource Availability

Lead contact

Further information and requests for reagents may be directed to the Lead contact Bin Qi (qb@yun.edu.cn).

Materials availability

All reagents and strains generated by this study are available through request to the lead contact with a completed Material Transfer Agreement.

Data and code availability

This paper does not report original code.

Any additional information required to reanalyze the data reported in this paper is available from the lead contact upon request (qb@ynu.edu.cn).

Experimental model and subject details

C. elegans strains and maintenance

Nematode stocks were maintained on nematode growth medium (NGM) plates seeded with bacteria (*E. coli* OP50) at 20˚C.

The following strains/alleles were obtained from the Caenorhabditis Genetics Center (CGC) or as indicated:

1) The following strains were obtained from CGC:

N2 Bristol (wild-type control strain);

AU3: *nsy-1(ag3)*;

ZD101: *tir-1(qd4)*;

RB1971: *bcf-1(ok2599)*;

KU25: *pmk-1(km25)*;

KU4: *sek-1(km4)*;

CX3695: *str-2::gfp+lin-15(+)*; shared from Huanhu Zhu lab

CX4998: *str-2::gfp+lin-15(+);nsy-1(ky397)*; shared from Hongyun Tang lab

2) The following strains were obtained from published papers.

PHX4067: [*Pbcf-1::bcf-1::gfp::3xflag*](He et al., 2023);

3) **The following strains were constructed by this study:**

YNU238: *nsy-1(ylf6)*, EMS mutant;

YNU186: [*Pnsy-1::gfp*;*Podr-1::rfp*] was constructed by injecting plasmid *Pnsy-1::nsy-1::gfp* with *Podr-1::rfp* in N2 background;

YNU465: [*Podr-1::nsy-1::gfp;Podr-1::rfp;nsy-1(ag3)*] was constructed by injecting plasmid *Podr-1::nsy-1::gfp* with *Podr-1::rfp* in *nsy-1(ag3)* background;

YNU491: AWC neuron specific knock out *nsy-1* strain was constructed by injecting plasmid pDD162[P*odr-1::Cas9*+P*u6::nsy-1-sg*], *nsy-1* repair template (synthesis from Tsingke), pDD162[P*eft-3::Cas9*+ P*u6::dpy-10-sg*], dpy-10 repair template(synthesis from Tsingke) in PHX4067(P*bcf-1::bcf-1::gfp::3xflag*) background.

YNU488: [*Pstr-130::str-130::mcherry*;*Podr-1::rfp*;*nsy-1(ag3)*] was constructed by injecting plasmid *Pstr-130::str-130::mcherry* with *Podr-1::rfp* in *nsy-1(ag3)* background;

YNU189: *Pbcf-1::bcf-1::gfp::3xflag;nsy-1(ag3)* was constructed by crossing PHX4067[*Pbcf-1::bcf-1::gfp::3xflag*] with AU3[*nsy-1(ag3)*];

YNU501: *nsy-1(ag3)*;*bcf-1(ok2599)* double mutant was constructed by crossing RB1971[*bcf-1(ok2599)*] with AU3[*nsy-1(ag3)*];

YNU517: *nsy-1(ag3);daf-2(e1370)* double mutant was constructed by crossing CB1370[*daf-2(e1370)*] with AU3[*nsy-1(ag3)*];

YNU508: [*Pstr130::str-130::mcherry;Podr-1::rfp;nsy-1(ag3)*] was constructed by injecting plasmid *Pstr130::str-130::mcherry* with *Podr-1::rfp* in *str-2::gfp+lin-15(+)* background.

Bacteria Strains

E. coli-OP50 (from Caenorhabditis Genetics Center (CGC)), and *Staphylococcus. Saprophyticus* (from ATCC) were cultured at 37°C in LB medium. A standard overnight cultured bacteria was then spread onto each Nematode growth media (NGM) plate.

Method Details

Generation of transgenic strains

1）To construct the *C. elegans* plasmid for expression of *nsy-1*, 1527bp promoter of *nsy-1* was inserted into the pPD95.77 vector. DNA plasmid mixture containing P*nsy-1::GFP* (20ng/ul) and P*odr-1p::RFP*(50ng/ul) was injected into the gonads of adult wild-type N2 animals.

2）To construct the *C. elegans* plasmid for expression of *nsy-1* in AWC neuron,

1348bp promoter of *odr-1* and genomic DNA of *nsy-1* was inserted into the pPD49.26 vector. DNA plasmid mixture containing P*odr-1::nsy-1::GFP* (20ng/ul) and P*odr-1::RFP* (50ng/ul) was injected into the gonads of adult *nsy-1(ag3)*.

3）To construct the *C. elegans* plasmid for expression of *str-130*, 2000bp promoter of *str-130* and 1324bp genomic DNA of *str-130* was inserted into the pPD49.26-mcherry vector. DNA plasmid mixture containing P*str-130::str-130::mcherry*(20ng/μl) and P*odr-1::rfp* (50ng/μl) was injected into the gonads of adult CX3695[*str-2::gfp+lin-15(+)*].

Generation *nsy-1* AWC neuron specific knock out strain and Genotyping.

To construct the *C. elegans* plasmid for knock out of *nsy-1* in AWC neuron, 600bp promoter of *eft-3* was replaced by 1348bp promoter of *odr-1* and *nsy-1* sgRNA was also inserted into the same CRISPR-Cas9-sgRNA vector pDD162 (Dickinson et al., 2013). The Cas9 target sites were designed via CRISPR design tool (http://crispor.tefor.net/) and the sgRNA sequences was 5'-GAATTTACGCGTTCGAGAAATGG-3'. Knockout strains were generated by injecting 25ng/μl Cas9-sgRNA plasmid, 2μM repair template, co-injection markers include 20ng/μl *dpy-10* Cas9-sgRNA plasmid and 2μM *dpy-10* repair template.

Worms were picked into 10 μl of worm lysis buffer (50 mM KCl,10 mM Tris-HCl pH 8.0, 2.5 mM $MgCl_2$, 0.45% NP40, 0.45% Tween-20, 0.01% Gelactin, 0.2 mg/mL Proteinase K), quickly freeze-thaw three times using liquid nitrogen, incubated it at 60°C for 90min and 95 °C for 20min. 1μl supernatant was taken and performed for PCR analysis with the following primers:

nsy-1: forward 5′-CAAGAGGCAAGTGCAGCATA-3′, reverse 5′-TGACTGTCCCATGCTCTCAC-3′, then digested with NheI endonuclease overnight and identified by DNA agarose electrophoresis.

Preparation of *Staphylococcus. Saprophyticus* (SS)

SS preparation was followed by our published protocol (Geng et al., 2022; Liu and Qi, 2023). Briefly, a standard overnight culture of SS (37℃ in LB broth) was diluted into fresh LB broth (1:100ratio). SS was then spread onto each NGM plate when the diluted bacteria grew to OD600 = 0.5.

Analysis of worm's growth in SS bacteria

The standard overnight cultured SS was then spread onto 60mm NGM plate. Worms were grown on *E. coli*-OP50, and eggs were collected by bleaching and then washing in M9 buffer. Synchronized L1 larvae were obtained by allowing the eggs to hatch in

M9 buffer for 12 hr. Synchronized L1s were seeded to plates prepared for the specific assay and incubated at 20℃ for 4 days. The developmental conditions were determined by body length.

Food behavior assay

1) Food avoidance assay

Food avoidance assay was performed following to our published methods (Qi et al., 2017). Briefly, 5ul of overnight cultured bacteria was seeded on the center of 60mm NGM plates. About 30-50 synchronized L1 animals were seeded onto the bacterial lawns and cultured at 20℃ for 8hr. The aversion index was determined by N(out of lawn)/N(total).

2) Food choice assay

Food choice assay was performed following to our published methods (Qi et al., 2017). Briefly, 5ul of overnight cultured bacteria was seeded on the different side of 60mm NGM plates. About 300 synchronized L1 animals were seeded onto the center of NGM plates and cultured at 20℃ for 8hr. The food trend index was determined by N (selecting food1)/ [N(selecting food1)+N(selecting food2)] and N(selecting food2)/[N(selecting food1)+N(selecting food2)].

Lifespan analysis

Larval Lifespan

Studies of larval lifespan were performed on NGM plates at 20℃ as previously described (Cui et al., 2013). Briefly, L1 staged worms were placed NGM plates or SS seeded NGM plates. Worms were scored every day. Prism8 software was used for statistical analysis.

Adult Lifespan

Studies of lifespan were performed on NGM plates at 20℃ as previously described (Kimura et al., 1997).

Briefly, lifespan was begun on day zero by placing healthy L4 stage hermaphrodites onto OP50 seeded NGM plates. Animals were transferred to a fresh OP50 or SS seeded plates during the reproductive period (approximately the first ten days) to eliminate self-progeny and every 2 days thereafter. Worms were scored every day. Prism8 software was used for statistical analysis.

EMS mutagenesis

Synchronized L1 animals were grown to the L4 stage on OP50 and then subjected to a

4-hour treatment with 0.5% EMS (Ethyl Methanesulfonate). After treatment, the P0 generation animals were thoroughly washed with M9 solution and transferred to OP50 plates to grow and produce the F1 generation. Groups of 3-4 F1 animals were picked and placed onto new OP50 plates (3-4 F1 worms per plate) to generate the F2 generation through self-fertilization. Once the F2 generation reached adulthood, all the F2 animals were bleached to obtain the next generation of eggs. Synchronized L1 larvae were obtained by allowing the eggs to hatch in M9 buffer for 12 hours. The synchronized L1s were then seeded onto SS plates and incubated at 20℃ for 4 days. Candidate mutants that could grow on SS plates were identified. To confirm the suspected mutants, each candidate mutant was picked singly onto OP50 for passaging and growth to adulthood. These adult animals were then bleached to obtain synchronized L1 mutants. The synchronized L1 mutants were seeded onto SS plates to confirm their ability to grow on SS.

Identification of EMS mutants

DNA isolation, library construction, and whole genome sequencing with gene identified were carried out according to the published protocol (Joseph et al., 2018).

i) Preparation of samples for Whole-Genome-Sequencing (WGS)

For each backcross, wild-type males were crossed to mutant hermaphrodites, F1 cross-progeny animals were individually cloned and F2 variants and wild-types were isolated under SS feeding conditon. The variant strains and wild-type strains were mixed respectively to constitute the “DNA-pool” used as samples for WGS. Whole-genome sequencing of pooled F2 recombinants, homozygous for the mutant phenotype following two outcrosses to wild-type N2 animals, was performed to identify the mutations.

ii) WGS data processing

For Whole-Genome-Sequencing, paired-end libraries were sequenced on an Illumina HiSeq 2000. Fastqc was used to control the quality of raw data and Trimmomatic was used to filter the data. Bwa was used to construct the index of *C.elegans* genome and align clean reads to the reference gene sequence (Species: *Caenorhabditis_elegans*; Source: UCSC; Reference Genome Version: WBcel235/ce11). The Samtools was used for file format conversion and sorting. Picard was used to remove the duplicate reads and then GATK was used to identify the intervals and realign. The realigned sequence was piled up by Samtools and then inputted to Varscan to call the variants including

SNPs and INDELs. Vcflib was used to perform subtraction between the wild-types and variants. The file was annotated by Snpeff and the candidate genes was finally obtained.

Preparation of samples for RNA sequencing

RNA-seq was done with three biological replicates that were independently generated, collected, and processed. Adult wild type (N2) or *nsy-1* mutant worms were bleached and then the eggs were incubated in M9 for 18 hours to obtain synchronized L1 worms. Synchronized L1 worms were cultured in the NGM plate seeded with OP50 or SS for 4hrs at 20°C. L1 worms were then collected for sequencing.

Fluorescence microscopy of *C. elegans*

Slides for imaging were prepared by making a fresh flattened 5% agarose pad. Worms were mounted on 5% agar pads in M9 buffer with 5mM levamisolem then sealed beneath a 22x22mm coverglass. Imaging was done using an Olympus BX53 microscope with a DP80 camera. *str-2::gfp* or *bcf-1::gfp* expression was measured through imaging.

Microscopy

The fluorescence photographs were taken by Olympus BX53 microscope with a DP80 camera. Development statistics were taken by Olympus MVX10 dissecting microscope with a DP80 camera.

QUANTIFICATION AND STATISTICAL ANALYSIS

Quantification

Animals were randomly selected for fluorescent photography. The size of transgene worms was photographed by the Nomarski microscope and measured by ImageJ software. ImageJ software was used for quantifying fluorescence intensity of indicated animals, which was then normalized with control group.

Statistical analysis

All experiments were performed independently at least three times with similar results.

All statistical analyses were performed using the unpaired two-tailed Student's test. Statistical parameters are presented as mean ± SD, statistical significance (P<0.05, *, P < 0.01, **, P < 0.001, ***), and "n" (the number of worms counted). The Log rank (Mantel-Cox) test was used for lifespan assay and the exact p values of statistics for all survival assays are listed in the Figure.

Reference:

Avery, J.A., Liu, A.G., Ingeholm, J.E., Gotts, S.J., and Martin, A. (2021). Viewing images of foods evokes taste quality-specific activity in gustatory insular cortex. Proc Natl Acad Sci U S A *118*.

Bargmann, C.I. (2006). Chemosensation in C. elegans. WormBook, 1-29.

Bargmann, C.I., Hartwieg, E., and Horvitz, H.R. (1993). Odorant-selective genes and neurons mediate olfaction in C. elegans. Cell *74*, 515-527.

Baugh, L.R., and Sternberg, P.W. (2006). DAF-16/FOXO regulates transcription of cki-1/Cip/Kip and repression of lin-4 during C. elegans L1 arrest. Curr Biol *16*, 780-785.

Buck, L., and Axel, R. (1991). A novel multigene family may encode odorant receptors: a molecular basis for odor recognition. Cell *65*, 175-187.

Chuang, C.F., and Bargmann, C.I. (2005). A Toll-interleukin 1 repeat protein at the synapse specifies asymmetric odorant receptor expression via ASK1 MAPKKK signaling. Gene Dev *19*, 270-281.

Chuang, C.F., VanHoven, M.K., Fetter, R.D., Verselis, V.K., and Bargmann, C.I. (2007). An innexin-dependent cell network establishes left-right neuronal asymmetry in
. Cell *129*, 787-799.

Cui, M., Cohen, M.L., Teng, C., and Han, M. (2013). The tumor suppressor Rb critically regulates starvation-induced stress response in C. elegans. Curr Biol *23*, 975-980.

Dickinson, D.J., Ward, J.D., Reiner, D.J., and Goldstein, B. (2013). Engineering the genome using Cas9-triggered homologous recombination. Nat Methods *10*, 1028-+.

Felix, M.A., and Braendle, C. (2010). The natural history of Caenorhabditis elegans. Curr Biol *20*, R965-R969.

Fiala, A. (2007). Olfaction and olfactory learning in Drosophila: recent progress. Curr Opin Neurobiol *17*, 720-726.

Florsheim, E.B., Bachtel, N.D., Cullen, J.L., Lima, B.G.C., Godazgar, M., Carvalho, F., Chatain, C.P., Zimmer, M.R., Zhang, C.L., Gautier, G.*, et al.* (2023). Immune sensing of food allergens promotes avoidance behaviour. Nature *620*, 643-+.

Florsheim, E.B., Sullivan, Z.A., Khoury-Hanold, W., and Medzhitov, R. (2021). Food allergy as a biological food quality control system. Cell *184*, 1440-1454.

Geng, S., Li, Q., Zhou, X., Zheng, J., Liu, H., Zeng, J., Yang, R., Fu, H., Hao, F., Feng, Q.*, et al.* (2022). Gut commensal E. coli outer membrane proteins activate the host food digestive system through neural-immune communication. Cell Host Microbe.

Hao, F.R., Liu, H.M., and Qi, B. (2024). Bacterial peptidoglycan acts as a digestive signal mediating host adaptation to diverse food resources in. Nat Commun *15*.

He, Y., Hao, F., Fu, H., Tian, G., Zhang, Y., Fu, K., and Qi, B. (2023). N-glycosylated intestinal protein BCF-1 shapes microbial colonization by binding bacteria via its fimbrial protein. Cell Rep *42*, 111993.

871 Hukema, R.K., Rademakers, S., Dekkers, M.P., Burghoorn, J., and Jansen, G. (2006). Antagonistic
872 sensory cues generate gustatory plasticity in Caenorhabditis elegans. Embo J *25*, 312-322.
873 Joseph, B.B., Blouin, N.A., and Fay, D.S. (2018). Use of a Sibling Subtraction Method for Identifying
874 Causal Mutations in Caenorhabditis elegans by Whole-Genome Sequencing. G3 (Bethesda) *8*,
875 669-678.
876 Julius, D., and Nathans, J. (2012). Signaling by sensory receptors. Cold Spring Harbor perspectives in
877 biology *4*, a005991.
878 Kim, D.H., Feinbaum, R., Alloing, G., Emerson, F.E., Garsin, D.A., Inoue, H., Tanaka-Hino, M., Hisamoto,
879 N., Matsumoto, K., Tan, M.W.*, et al.* (2002). A conserved p38 MAP kinase pathway in Caenorhabditis
880 elegans innate immunity. Science *297*, 623-626.
881 Kimura, K.D., Tissenbaum, H.A., Liu, Y.X., and Ruvkun, G. (1997). daf-2, an insulin receptor-like gene
882 that regulates longevity and diapause in Caenorhabditis elegans. Science *277*, 942-946.
883 Kodama, E., Kuhara, A., Mohri-Shiomi, A., Kimura, K.D., Okumura, M., Tomioka, M., Iino, Y., and Mori, I.
884 (2006). Insulin-like signaling and the neural circuit for integrative behavior in C. elegans. Genes Dev *20*,
885 2955-2960.
886 Liu, H., and Qi, B. (2023). Protocol for investigating the effect of food digestion in C. elegans on
887 development by feeding the inedible bacteria Staphylococcus saprophyticus. STAR Protoc *4*, 101990.
888 Liu, P., Liu, X., and Qi, B. (2024). UPRER–immunity axis acts as physiological food evaluation system
889 that promotes aversion behavior in sensing low-quality food. Elife *13:RP94181*.
890 Matsunaga, Y., Matsukawa, T., Iwasaki, T., Nagata, K., and Kawano, T. (2018). Comparison of
891 physiological functions of antagonistic insulin-like peptides, INS-23 and INS-18, in. Biosci Biotech Bioch
892 *82*, 90-96.
893 McLachlan, I.G., Kramer, T.S., Dua, M., DiLoreto, E.M., Gomes, M.A., Dag, U., Srinivasan, J., and Flavell,
894 S.W. (2022). Diverse states and stimuli tune olfactory receptor expression levels to modulate
895 food-seeking behavior. Elife *11*.
896 Plum, T., Binzberger, R., Thiele, R., Shang, F.W., Postrach, D., Fung, C., Fortea, M., Stakenborg, N., Wang,
897 Z., Tappe-Theodor, A.*, et al.* (2023). Mast cells link immune sensing to antigen-avoidance behaviour.
898 Nature *620*, 634-+.
899 Qi, B., Kniazeva, M., and Han, M. (2017). A vitamin-B2-sensing mechanism that regulates gut protease
900 activity to impact animal's food behavior and growth. Elife *6*.
901 Ryu, L., Cheon, Y., Huh, Y.H., Pyo, S., Chinta, S., Choi, H., Butcher, R.A., and Kim, K. (2018). Feeding state
902 regulates pheromone-mediated avoidance behavior via the insulin signaling pathway in. Embo J *37*.
903 Sagasti, A., Hisamoto, N., Hyodo, J., Tanaka-Hino, M., Matsumoto, K., and Bargmann, C.I. (2001). The
904 CaMKII UNC-43 activates the MAPKKK NSY-1 to execute a lateral signaling decision required for
905 asymmetric olfactory neuron fates. Cell *105*, 221-232.
906 Samuel, B.S., Rowedder, H., Braendle, C., Felix, M.A., and Ruvkun, G. (2016). Caenorhabditis elegans
907 responses to bacteria from its natural habitats. P Natl Acad Sci USA *113*, E3941-E3949.
908 Schulenburg, H., and Felix, M.A. (2017). The Natural Biotic Environment of Caenorhabditis elegans.
909 Genetics *206*, 55-86.
910 Scott, K. (2018). Gustatory Processing in Drosophila melanogaster. Annu Rev Entomol *63*, 15-30.
911 Sengupta, P., Chou, J.H., and Bargmann, C.I. (1996). odr-10 encodes a seven transmembrane domain
912 olfactory receptor required for responses to the odorant diacetyl. Cell *84*, 899-909.
913 Troemel, E.R., Chou, J.H., Dwyer, N.D., Colbert, H.A., and Bargmann, C.I. (1995). Divergent seven
914 transmembrane receptors are candidate chemosensory receptors in C. elegans. Cell *83*, 207-218.

915 Troemel, E.R., Kimmel, B.E., and Bargmann, C.I. (1997). Reprogramming chemotaxis responses:
916 sensory neurons define olfactory preferences in C. elegans. Cell *91*, 161-169.
917 Troemel, E.R., Sagasti, A., and Bargmann, C.I. (1999). Lateral signaling mediated by axon contact and
918 calcium entry regulates asymmetric odorant receptor expression in C. elegans. Cell *99*, 387-398.
919 Vidal, B., Aghayeva, U., Sun, H., Wang, C., Glenwinkel, L., Bayer, E.A., and Hobert, O. (2018). An atlas of
920 Caenorhabditis elegans chemoreceptor expression. Plos Biol *16*, e2004218.
921 Wes, P.D., and Bargmann, C.I. (2001). odour discrimination requires asymmetric diversity in olfactory
922 neurons. Nature *410*, 698-701.
923

Figure 1

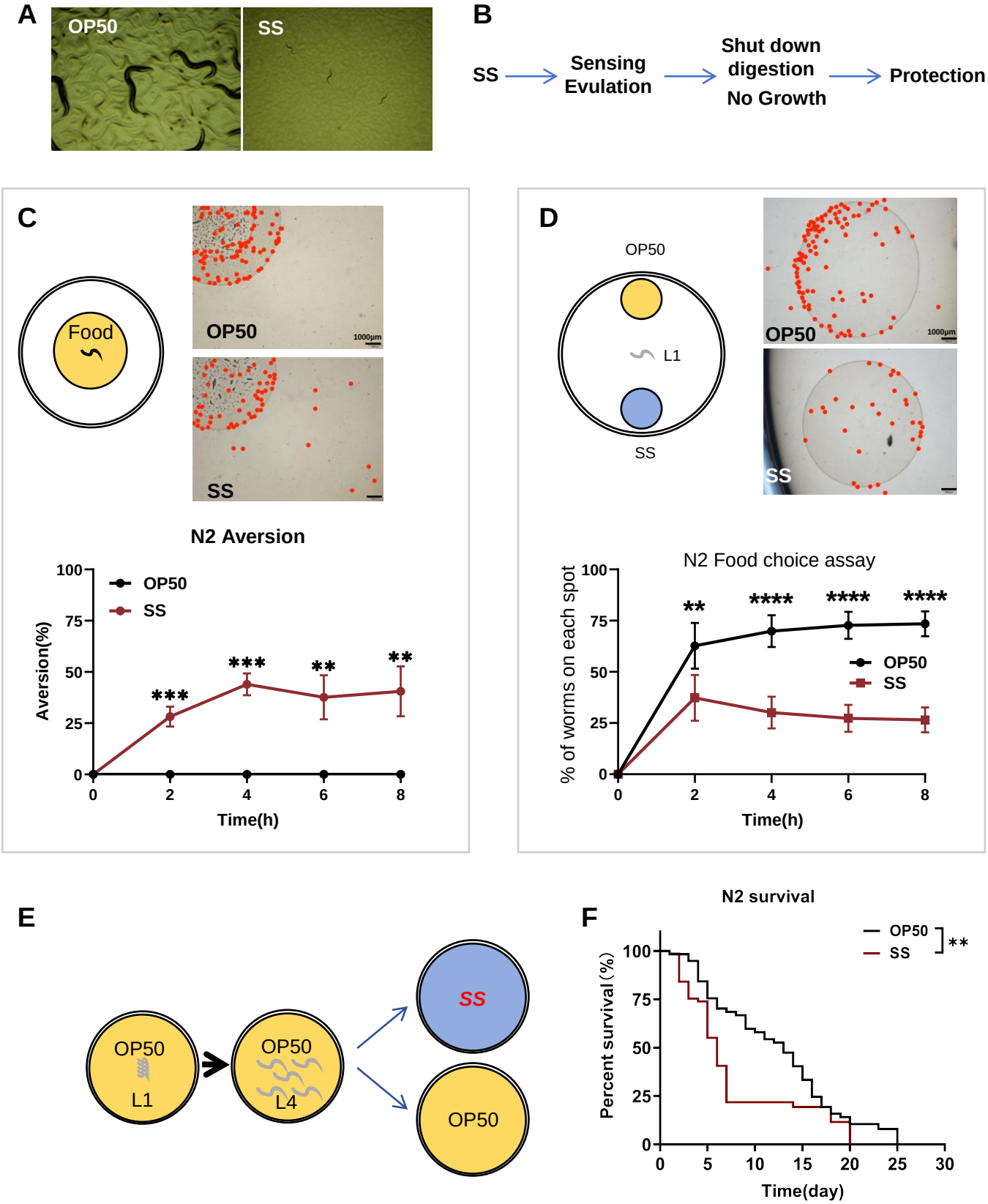
A
OP50
SS
B
SS
Sensing Evulation
Shut down digestion
No Growth
Protection
C
Food
OP50
SS
1000μm
N2 Aversion
Aversion(%)
Time(h)
OP50
SS
***
***
**
**
D
OP50
L1
SS
N2 Food choice assay
% of worms on each spot
Time(h)
**
****
****
****
E
OP50
L1
OP50
L4
SS
OP50
F
N2 survival
Percent survival (%)
Time(day)
OP50
SS
**

Figure 2

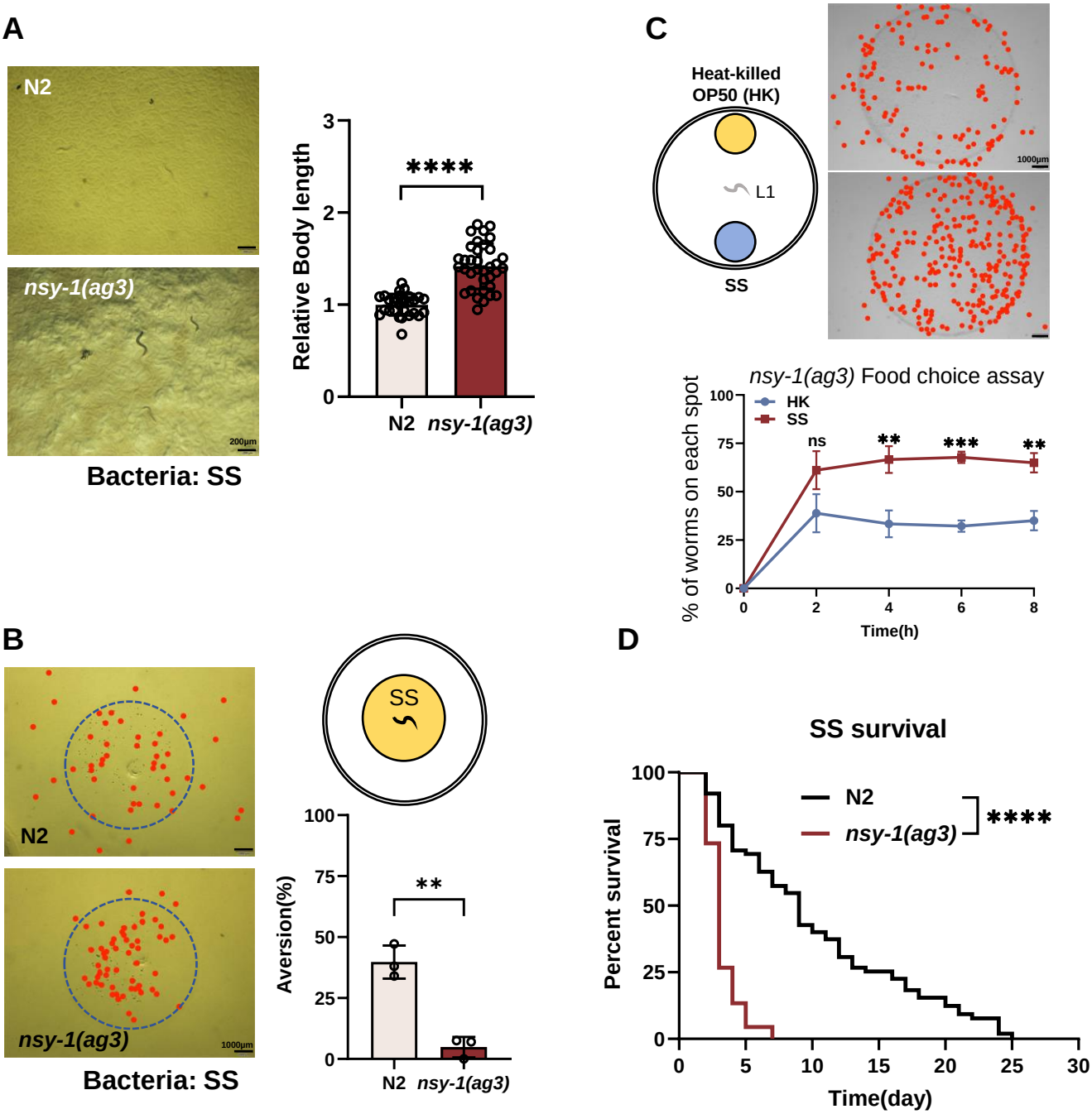
A
N2
nsy-1(ag3)
200μm
Bacteria: SS
Relative Body length
****
N2
nsy-1(ag3)
B
N2
nsy-1(ag3)
1000μm
Bacteria: SS
SS
Aversion(%)
**
N2
nsy-1(ag3)
C
Heat-killed
OP50 (HK)
L1
SS
1000μm
nsy-1(ag3) Food choice assay
HK
SS
% of worms on each spot
ns
**
***
**
Time(h)
D
SS survival
N2
nsy-1(ag3)
****
Percent survival
Time(day)

Figure 3

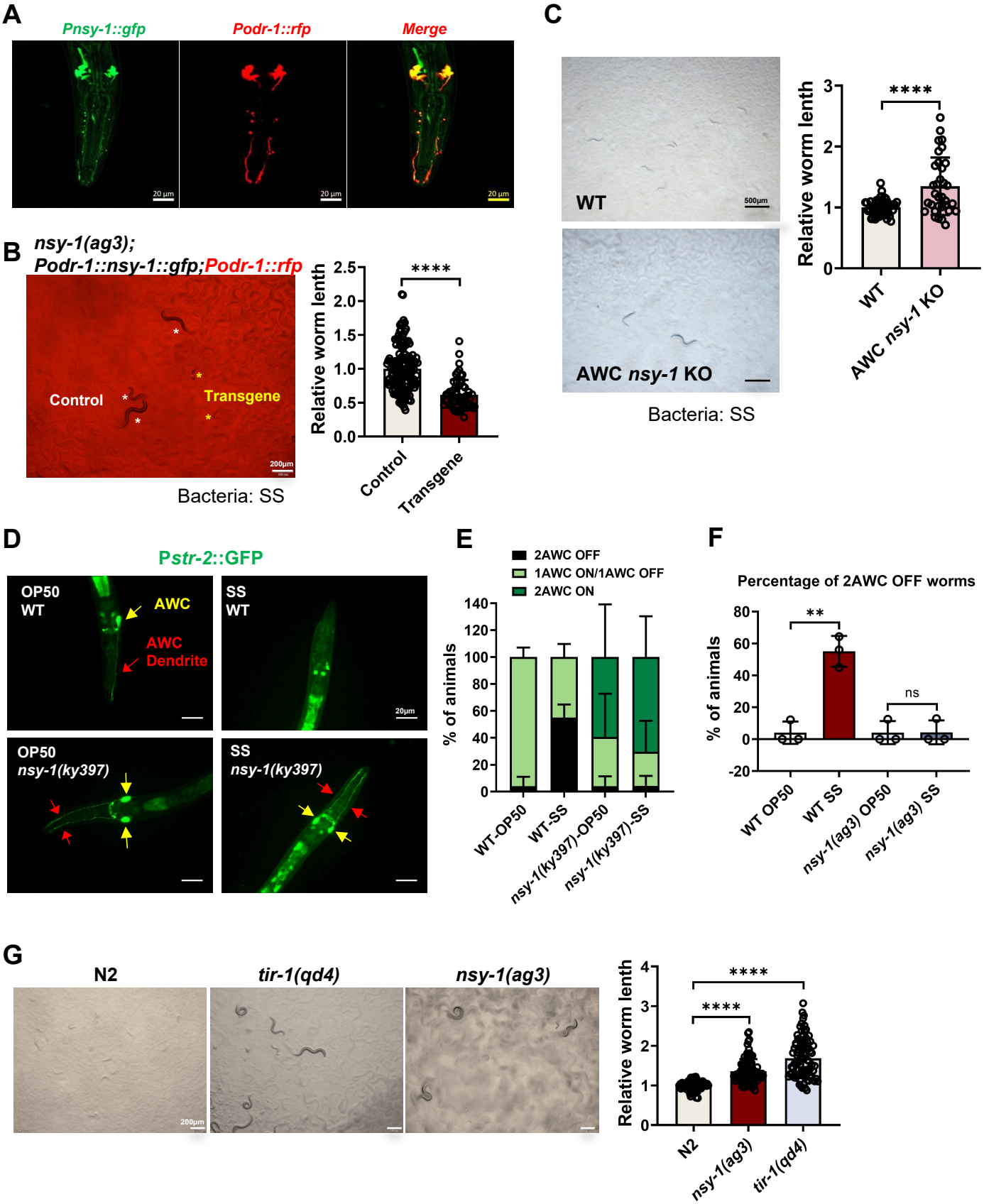
A
Pnsy-1::gfp
Podr-1::rfp
Merge
20 µm
B
nsy-1(ag3);
Podr-1::nsy-1::gfp;Podr-1::rfp
Control
Transgene
200µm
Bacteria: SS
Relative worm lenth
****
Control
Transgene
C
WT
500µm
AWC nsy-1 KO
Bacteria: SS
Relative worm lenth
****
WT
AWC nsy-1 KO
D
Pstr-2::GFP
OP50
WT
AWC
AWC
Dendrite
SS
WT
20µm
OP50
nsy-1(ky397)
SS
nsy-1(ky397)
E
2AWC OFF
1AWC ON/1AWC OFF
2AWC ON
% of animals
WT-OP50
WT-SS
nsy-1(ky397)-OP50
nsy-1(ky397)-SS
F
Percentage of 2AWC OFF worms
% of animals
**
ns
WT OP50
WT SS
nsy-1(ag3) OP50
nsy-1(ag3) SS
G
N2
tir-1(qd4)
nsy-1(ag3)
200µm
Relative worm lenth
****
****
N2
nsy-1(ag3)
tir-1(qd4)

Figure 4

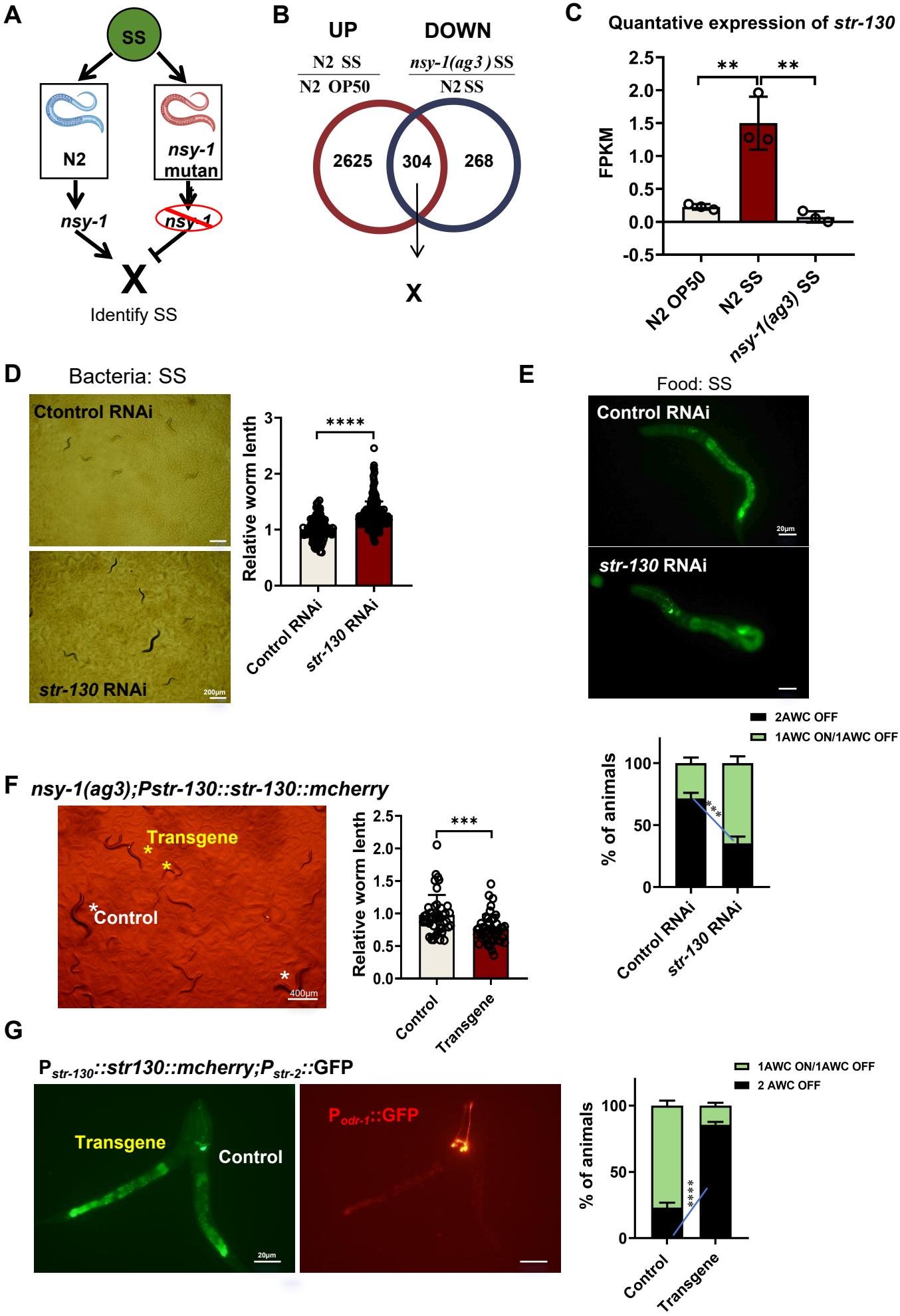
A
SS
N2
nsy-1 mutan
nsy-1
nsy-1
X
Identify SS
B
UP
DOWN
N2 SS
N2 OP50
nsy-1(ag3) SS
N2 SS
2625
304
268
X
C
Quantative expression of str-130
FPKM
2.5
2.0
1.5
1.0
0.5
0.0
-0.5
**
**
N2 OP50
N2 SS
nsy-1(ag3) SS
D
Bacteria: SS
Ctontrol RNAi
str-130 RNAi
200μm
Relative worm lenth
3
2
1
0
****
Control RNAi
str-130 RNAi
E
Food: SS
Control RNAi
20μm
str-130 RNAi
2AWC OFF
1AWC ON/1AWC OFF
% of animals
100
50
0
***
Control RNAi
str-130 RNAi
F
nsy-1(ag3);Pstr-130::str-130::mcherry
Transgene
Control
400μm
Relative worm lenth
2.5
2.0
1.5
1.0
0.5
0.0
***
Control
Transgene
G
Pstr-130::str130::mcherry;Pstr-2::GFP
Transgene
Control
20μm
Podr-1::GFP
1AWC ON/1AWC OFF
2 AWC OFF
% of animals
100
50
0
****
Control
Transgene

Figure 5

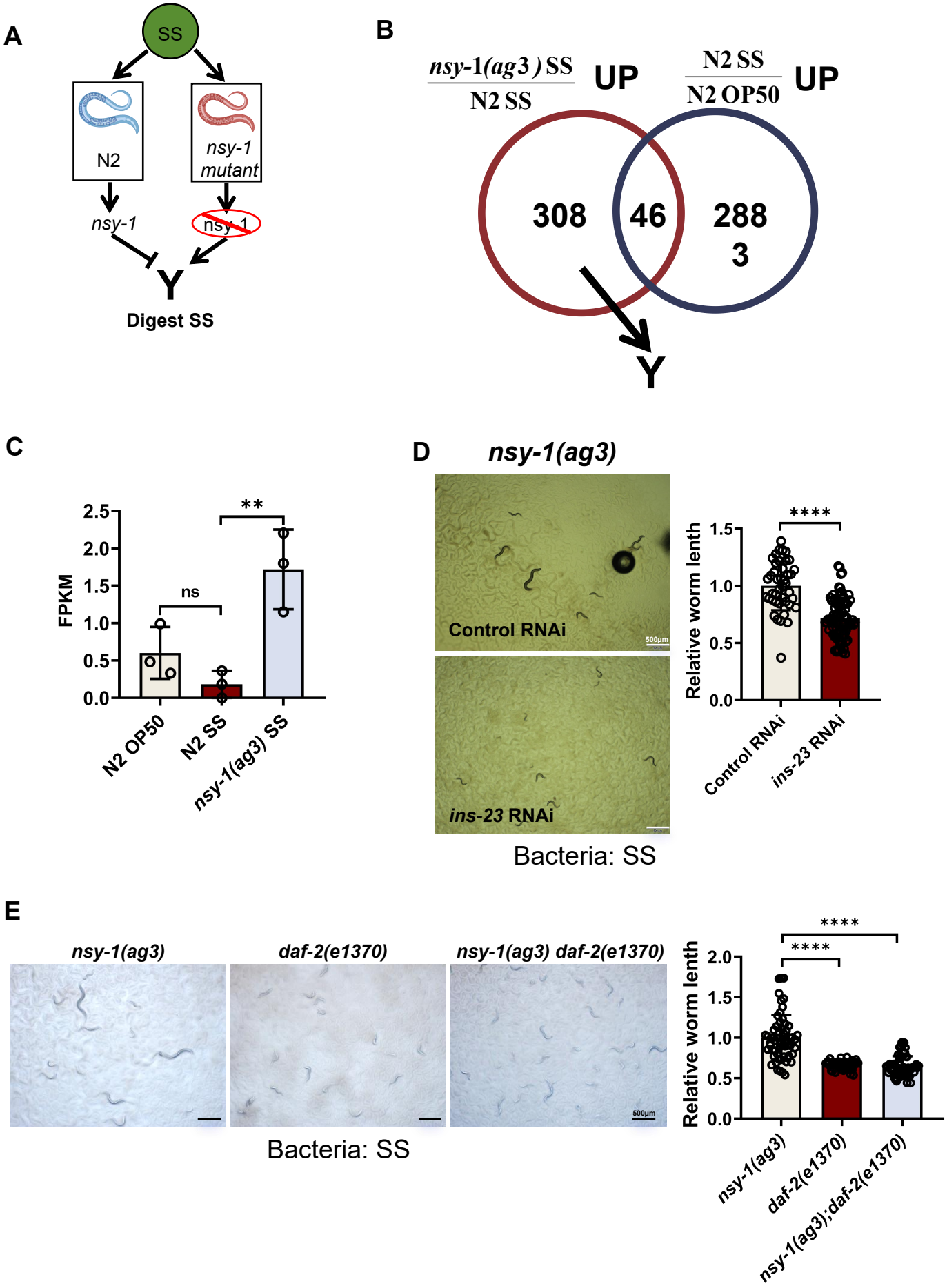
A
SS
N2
nsy-1 mutant
nsy-1
nsy-1
Y
Digest SS
B
nsy-1(ag3) SS / N2 SS
UP
N2 SS / N2 OP50
UP
308
46
288
3
Y
C
FPKM
2.5
2.0
1.5
1.0
0.5
0.0
ns
**
N2 OP50
N2 SS
nsy-1(ag3) SS
D
nsy-1(ag3)
Control RNAi
ins-23 RNAi
Relative worm lenth
****
Control RNAi
ins-23 RNAi
Bacteria: SS
E
nsy-1(ag3)
daf-2(e1370)
nsy-1(ag3) daf-2(e1370)
Bacteria: SS
Relative worm lenth
****
****
nsy-1(ag3)
daf-2(e1370)
nsy-1(ag3);daf-2(e1370)

Figure 6

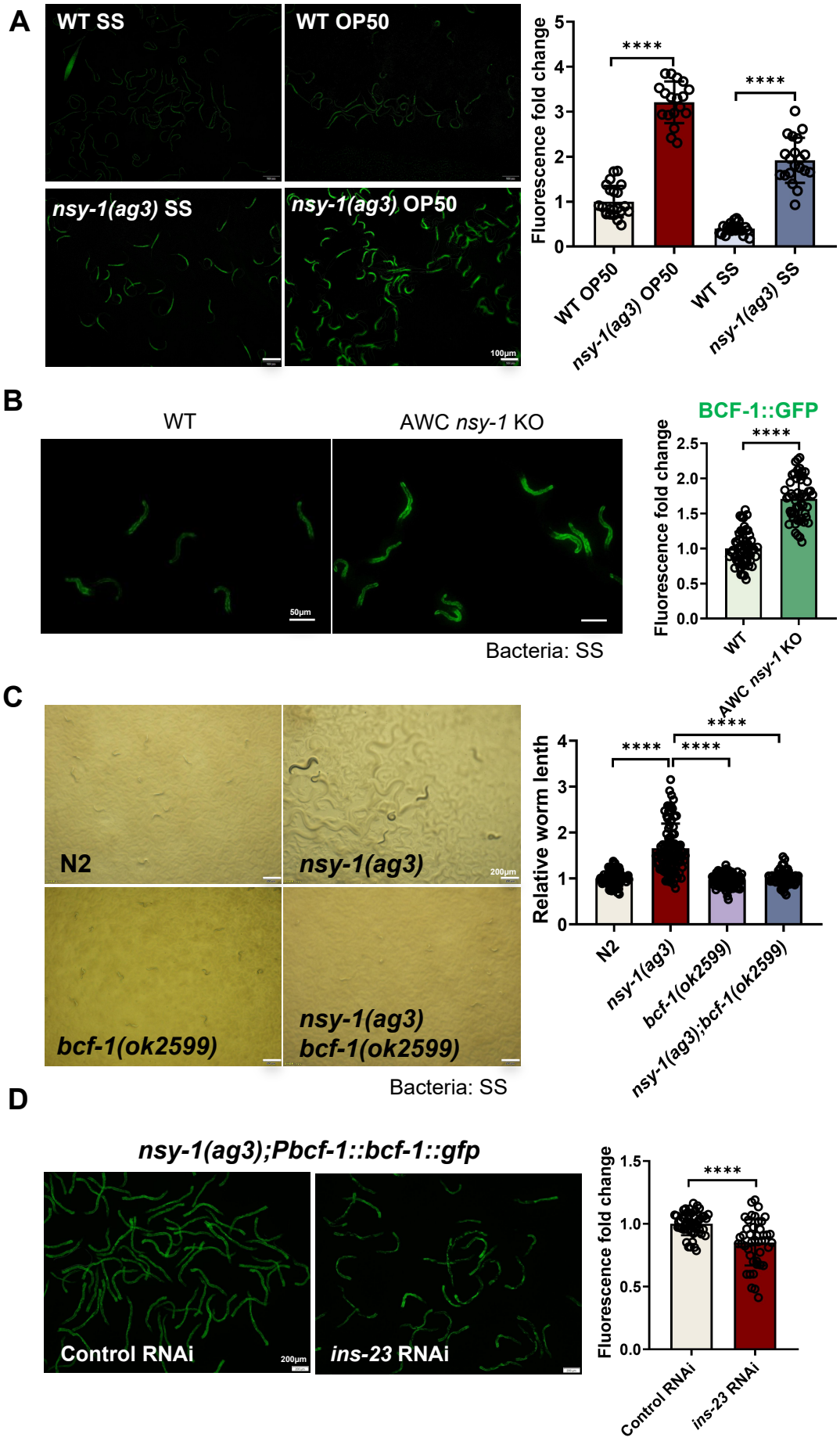
A
WT SS
WT OP50
nsy-1(ag3) SS
nsy-1(ag3) OP50
100μm
Fluorescence fold change
****
****
WT OP50
nsy-1(ag3) OP50
WT SS
nsy-1(ag3) SS
B
WT
AWC nsy-1 KO
50μm
Bacteria: SS
BCF-1::GFP
Fluorescence fold change
****
WT
AWC nsy-1 KO
C
N2
nsy-1(ag3)
200μm
bcf-1(ok2599)
nsy-1(ag3)
bcf-1(ok2599)
Bacteria: SS
Relative worm lenth
****
****
****
N2
nsy-1(ag3)
bcf-1(ok2599)
nsy-1(ag3);bcf-1(ok2599)
D
nsy-1(ag3);Pbcf-1::bcf-1::gfp
Control RNAi
200μm
ins-23 RNAi
Fluorescence fold change
****
Control RNAi
ins-23 RNAi

Figure 7

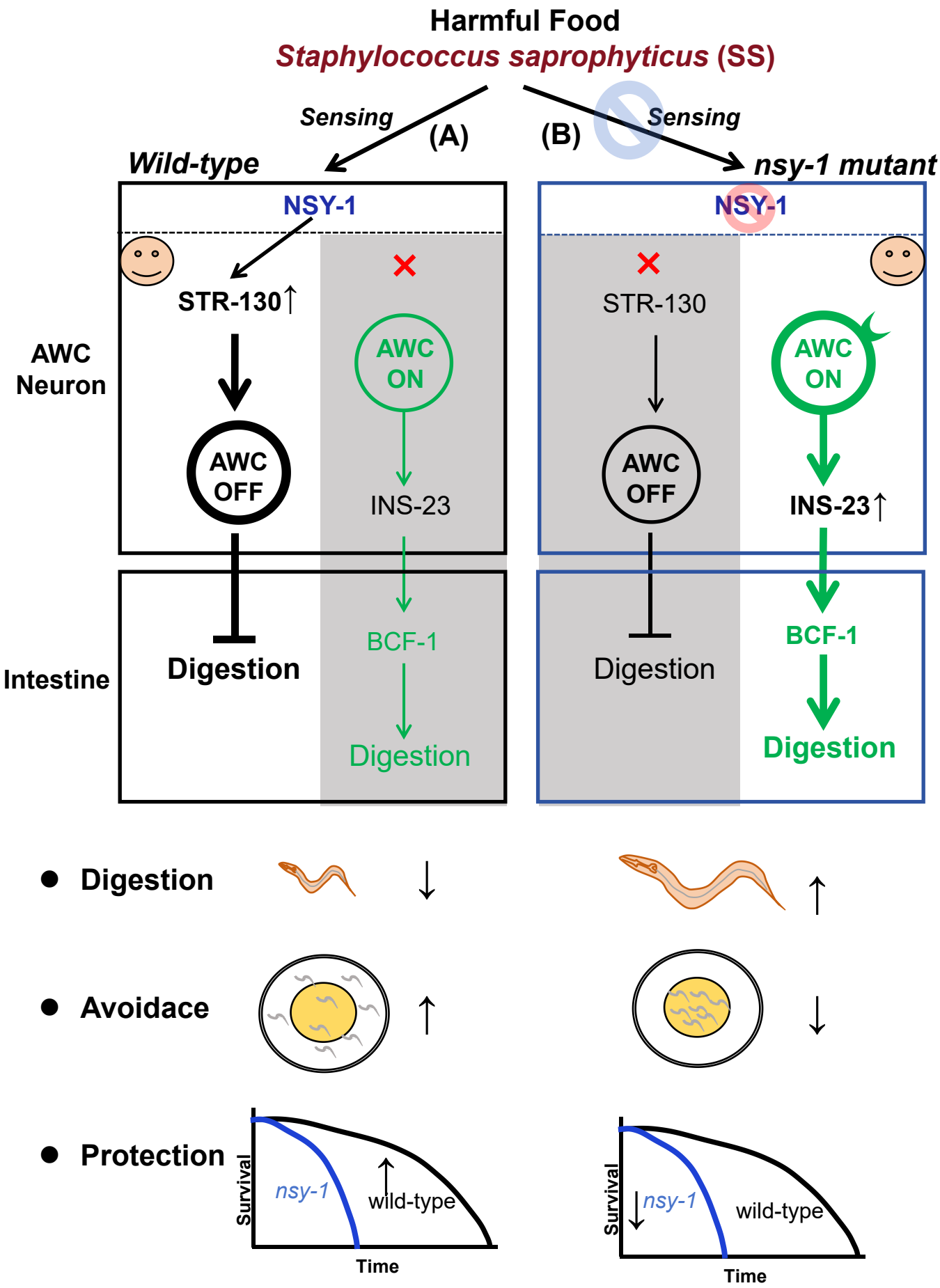
Harmful Food
Staphylococcus saprophyticus (SS)
Sensing
(A)
(B)
Sensing
Wild-type
nsy-1 mutant
NSY-1
NSY-1
STR-130↑
STR-130
AWC Neuron
AWC ON
AWC OFF
INS-23
AWC ON
AWC OFF
INS-23↑
Intestine
Digestion
BCF-1
Digestion
Digestion
BCF-1
Digestion
Digestion
Avoidace
Protection
Survival
nsy-1
wild-type
Time
Survival
nsy-1
wild-type
Time